Journal of Computer-Aided Materials Design manuscript No.
(will be inserted by the editor)

A Multilattice Quasicontinuum for Phase Transforming Materials: Cascading Cauchy Born Kinematics

M. Dobson · R. S. Elliott · M. Luskin · E. B. Tadmor

March 26, 2007

Abstract The quasicontinuum (QC) method is applied to materials possessing a multilattice crystal structure. Cauchy-Born (CB) kinematics, which accounts for the shifts of the crystal basis, is used in continuum regions to relate atomic motions to continuum deformation gradients. To avoid failures of the CB kinematics, QC is augmented with a phonon stability analysis that detects lattice period extensions and identifies the minimum required periodic cell size. This augmented approach is referred to as *Cascading Cauchy-Born kinematics*. The method is analyzed for both first- and second-order phase transformations, and demonstrated numerically on a one-dimensional test problem.

Keywords multiscale, quasicontinuum, multilattice, cascading Cauchy-Born, finite elements

1 Introduction

The quasicontinuum (QC) method [1–3] is a multiscale method coupling an atomistic region with a surrounding continuum region modeled within a nonlinear finite element formulation. The constitutive response in the continuum is obtained by the application of Cauchy-Born (CB) kinematics to the underlying lattice and calculation of the energy and necessary gradients using the same inter-atomic potentials applied in the atomistic region. This, together with built-in automatic mesh refinement, lends to QC a seamlessness and adaptivity that facilitates the simulation of complex boundary-value problems (BVPs).

In the application of QC to multifunctional materials, such as ferroelectrics or shape memory alloys, it must be recognized that these materials have multilattice

M. Dobson · M. Luskin
School of Mathematics, University of Minnesota, Minneapolis, MN 55455, USA

R. S. Elliott · E. B. Tadmor
Aerospace Engineering and Mechanics, University of Minnesota, Minneapolis, MN 55455, USA

E. B. Tadmor
Department of Mechanical Engineering, Technion – Israel Institute of Technology, 32000 Haifa, Israel

crystal structures. This means that CB kinematics, which for simple crystals states that the atoms are mapped according to the continuum field, must also account for the shifting of the basis atoms [4]. This is straightforward to do, however a question arises as to which description of the crystal structure should be used. Traditionally, CB kinematics has been interpreted as being applied to the *essential* description of the crystal, i.e., the simplest periodic structure that reproduces the crystal structure (see [5,6] and references there-in). This was the approach adopted in the multilattice QC implementation of Tadmor *et al.* [7] that was later applied to a number of problems of interest [8,9]. However, as pointed out by Pitteri [5] and Zanzotto [6,10,11], the traditional definition of CB kinematics can fail in a number of ways. In particular, some deformations require an increase in the periodic size of the unit cell. The problem is that the appropriate cell size for a particular BVP cannot be known *a priori* and in fact, it is likely to vary depending on the spatial location for the case of non-uniform deformation. Allowing such period extensions can be critical in many cases where phase transformations occur in the material.

In this paper we propose a novel solution to this problem. Rather than applying the CB kinematics to a static representation of the lattice structure, the lattice representation is dynamically updated using an algorithm designed to detect energetically favorable unit cell extensions during the simulation. This is achieved by performing a phonon stability analysis, along the lines proposed by Elliott et al. [12,13], locally within each finite element in the continuum region at the end of each QC load step. This analysis detects the onset of period extension and recursively identifies a new physically appropriate lattice description. We refer to this approach as "Cascading Cauchy-Born" (CCB) kinematics.

The remainder of the paper is as follows. In Section 2, a brief review of QC for simple and multilattice crystals is presented. Section 3 introduces the CCB kinematics technique and describes conditions under which it will detect energetically favorable phase transformations. Section 4 presents a simple one-dimensional (1D) material model that clearly illustrates its necessity. Finally, in Section 5, a brief discussion of related issues left to future work is presented.

2 One-dimensional quasicontinuum method

In this section a brief overview of the QC methodology is presented. The reader is referred to [2,3] for more details. Since the examples in this paper are 1D, the discussion is limited to that simplified special case.

2.1 One-dimensional crystals

In 1D, a lattice is defined by the set of positions ℓa_0, where $\ell \in \{-\infty, \ldots, \infty\}$ is an integer index and a_0 is the reference lattice parameter (or the unit cell length). A crystal possessing a simple-lattice structure is one where a single atom is associated with each lattice site. The positions of the atoms in the reference configuration are then

$$X[\ell] = \ell a_0. \tag{1}$$

Multilattice crystals are obtained by placing a basis of $N_B^0 > 1$ atoms at each lattice site. The superscript 0 indicates that this is an initial choice for the basis size that may

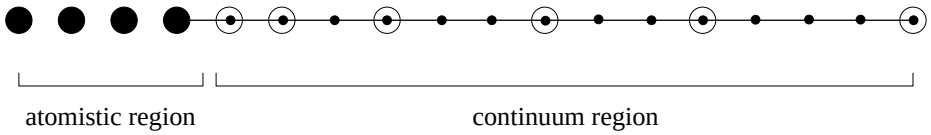

Fig. 1 A 1D QC model for a simple lattice. The filled circles are nonlocal repsites (which for a simple lattice correspond to atoms), the open circles are local repsites and the the dots denote the underlying lattice. The lines represent the elements defined in the continuum region.

be increased later by the CCB approach. In this case the positions of the atoms in the reference configuration are given by

$$X \begin{bmatrix} \ell \\ \alpha \end{bmatrix} = \ell a_0 + \Delta_\alpha, \qquad \alpha \in \{1, ..., N_B^0\}, \tag{2}$$

where Δ_α are additional *reference shifts* locating the basis atoms relative to the lattice site in the reference configuration. Without loss of generality, we set $\Delta_1 = 0$, i.e., the first basis atom is located at the lattice site.

The above definitions assume an essential description of the crystal structure. Of course, it is always possible to describe a simple crystal as a multilattice crystal with a unit cell containing more than one atom. Similarly, multilattice crystals can be described by unit cells and bases of different sizes. These non-essential descriptions allow for more complicated deformations including many types of phase transformations. This is discussed further in Section 3, but first we describe the application of QC to simple and multilattice crystals.

2.2 QC for simple crystals

Consider a 1D simple crystal consisting of N lattice sites ($= N$ atoms) loaded by applied displacements and/or external loads. The objective is to compute the equilibrium configuration associated with this applied loading. In QC, the computational burden associated with this is reduced by selecting a small subset of all lattice sites in the material as *representative sites* (or *repsites*)[1] that through appropriate weighted sums provide an adequate approximation for the energy of the complete system. The result of this representation is that the simulation domain is divided into an atomistic region where all sites are represented for a total of, n_a, *nonlocal*[2] repsites, and a continuum region where only a small number, n_c, of *local* repsites are retained (Fig. 1). The total number of repsites in the QC model is then $n = n_a + n_c$, where normally $n \ll N$. The repsites serve as the nodes in a finite element mesh containing n_e elements, which is used to compute deformation gradients in the continuum region.

[1] In the original QC formulation, the terms representative atoms and repatoms were used. Here the concept is generalized for multilattices by referring to representative lattice sites, each of which may be associated with one or more atoms.

[2] The term nonlocal indicates that the repsite participates in long-range interactions with its surrounding repsites, whereas local denotes interactions only with adjacent neighbor repsites. It is emphasized that all energy calculations are performed using the possibly long-ranged atomic potentials, but for local repsites only adjacent neighbor repsites are used to determine the deformation gradient.

The repsites have positions X^i $(= \ell^i a_0)$ in the reference configuration. They move in response to the applied loading to new positions,

$$x^i = X^i + u^i, \qquad i \in \{1, \ldots, n\}, \tag{3}$$

where u^i are displacements, and the standard continuum mechanics convention of using uppercase letters for measures in the reference configuration and lowercase letters for the deformed configuration is used. Equilibrium configurations are obtained by minimizing the total QC potential energy which is given as a sum of the atomistic energy, the continuum energy, and the load potential,

$$\Pi(\mathbf{u}) = \sum_{i=1}^{n_a} E^i(\mathbf{u}) + a_0 \sum_{e=1}^{n_e} \nu^e W(F^e(\mathbf{u})) - \sum_{j=1}^{n} \left(f^j_{\text{ext}} + f^j_{\text{ghost}} \right) u^j, \tag{4}$$

with respect to the set of repsite displacements, $\mathbf{u} = \{u^1, \ldots, u^n\}$, subject to prescribed boundary conditions.

The first term in (4) is the energy of the atomistic region taken as a sum over individual atom energies E^i. For example, the energy of atom i for a pair-potential model $\phi(r)$ is,

$$E^i(\mathbf{u}) = \frac{1}{2} \sum_{j=1}^{n} \phi(X^j + u^j - X^i - u^i), \tag{5}$$

where ϕ is assumed to be an even function (such as the Lennard-Jones potential in (29)) and to take a value of zero at $r = 0$ for simplicity of notation. The computation is simplified by applying a cutoff to the inter-atomic potential ϕ and ensuring that all lattice sites in the continuum region that are within the cutoff distance of the atomistic region are local repsites [14].

The second term in (4) is the energy of the continuum region taken as a sum over the strain energy of the elements. Here $W(F)$ is the strain-energy density (SED), that is, the energy per unit length of an infinite lattice subject to the deformation gradient, F, within the element:

$$F = 1 + \Delta u / h, \tag{6}$$

where Δu is the change of displacement across the element and h is its length in the reference configuration. In addition, ν^e is the number of lattice sites in element e represented by its local repsites.[3] In QC, $W(F)$ is computed using the same inter-atomic potential applied in the atomistic region by assuming CB kinematics to relate atomic motion in the lattice underlying the continuum to the deformation gradient F. For a simple lattice this is

$$x[\ell] = FX[\ell] = F\ell a_0, \tag{7}$$

where $x[\ell]$ is the position of the atom occupying site ℓ in the deformed configuration. The resulting SED function for a pair-potential is:

$$W(F) = \frac{1}{a_0} \sum_{\ell} \phi(F\ell a_0). \tag{8}$$

[3] For elements where both nodes are local repsites, $\nu = h/a$. However, for elements at the continuum/atomistic interface ν is equal to half the lattice sites in the element.

The third term in (4) is the potential of the external loads f^i_{ext} along with the ghost-force correction terms f^i_{ghost} [2] that cancel out the atomistic-continuum mismatch error at the interface.

QC simulations are performed by gradually applying boundary conditions and external forces in a sequence of quasi-static load steps. At each step, the load parameter—for instance external force or nominal strain—is incremented and the system is relaxed to satisfy the external conditions represented by the parameter. This incremental procedure helps to ensure that at each step, the previous step's equilibrium configuration is close to the current step's final relaxed state, making the computation stable.

2.3 QC for multilattice crystals

The multilattice implementation of QC is essentially identical to that given in the previous subsection with the exception of the following modifications. Nonlocal repsites must now represent the entire basis of atoms placed at their location. Thus in addition to the displacement of the repsite, the shifts δ^i_α $(\alpha = 1, \ldots, N_B)$ of the basis atoms located at nonlocal repsite i must be stored. In this manner, a degree of freedom is associated with every atom in the atomistic region. Note that here N_B indicates a current basis size, which may be larger than N^0_B as a result of CCB kinematics as explained in the next section. As before, without loss of generality we set $\delta^i_1 = 0$. The shifts are given relative to the repsite location, so that in the reference configuration $\delta^i_\alpha = \Delta^i_\alpha$. This representation is convenient for the analytical discussion that follows, but it is noted that a representation that takes the shifts to be relative to the reference shifts is often computationally advantageous.

In the continuum region, the shifts of the basis atoms are stored within the finite elements as internal variables. CB kinematics for multilattices states that

$$x \begin{bmatrix} \ell \\ \alpha \end{bmatrix} = F\ell a_0 + \delta_\alpha. \tag{9}$$

That is, all unit cells deform uniformly, but the basis atoms are free to displace relative to one another during the deformation. As a result, the multilattice SED function will depend on element shifts as well as the deformation gradient,

$$\begin{aligned} W(F, \boldsymbol{\delta}) &= \frac{1}{a} \sum_{\alpha=1}^{N_B} \sum_{\ell} \sum_{\beta=1}^{N_B} \phi_{\alpha\beta} \left(x \begin{bmatrix} \ell \\ \beta \end{bmatrix} - x \begin{bmatrix} 0 \\ \alpha \end{bmatrix} \right) \\ &= \frac{1}{a} \sum_{\alpha=1}^{N_B} \sum_{\ell} \sum_{\beta=1}^{N_B} \phi_{\alpha\beta}(F\ell a + \delta_\beta - \delta_\alpha), \end{aligned} \tag{10}$$

where ϕ can explicitly depend on α and β as is the case when multiple atomic species exist in the multilattice crystal. The SED accounts for the interaction of every atom in the current unit cell, indexed by α, with all other atoms in the infinite multilattice displaced according to (9), and is normalized by the reference length of the current unit cell, $a \equiv (N_B/N^0_B)a_0$. The dependence on $\boldsymbol{\delta} = \{\delta_1, \ldots, \delta_{N_B}\}$ can be minimized out locally (for instance, via a conjugate-gradient technique) [7],

$$\min_{\boldsymbol{\delta}} W(F, \boldsymbol{\delta}). \tag{11}$$

This implicitly defines the function $\boldsymbol{\delta}(F)$ that can be used to derive an effective SED that depends only on the deformation gradient,

$$\widetilde{W}(F) \equiv W(F, \boldsymbol{\delta}(F)). \tag{12}$$

3 Cascading Cauchy-Born (CCB) kinematics for multilattices

When using CB kinematics one inevitably must make a decision about the crystal basis that will be used. Most often an essential description is chosen for simplicity or lack of information pointing to a better candidate. In some cases though, such as when translation-symmetry breaking phase transformations occur, it is important to use a non-essential description [13]. In many studies, an arbitrary fixed choice for the unit cell is made at the outset, and often an investigation or discussion of the consequences of this choice is not presented.

In general, the appropriate description is *a priori* unknown and, in fact, it usually depends on the applied boundary conditions and the evolving deformation of the crystal. Therefore, in this work Cascading Cauchy-Born kinematics is employed. This set of kinematics, inspired by the procedure outlined in [13], starts with an essential basis description of the crystal for each continuum element but makes this basis a dynamic entity by monitoring the phonon stability of the crystal structure as its deformation evolves in response to applied loads. When a loss of stability indicating a phase transformation is detected, the basis size is increased as necessary to describe the new phase.

3.1 Phonon stability

The objective of the phonon stability analysis for CCB kinematics is to detect situations in which the total energy can be further reduced by adopting a larger basis in one or more of the finite elements. If this is possible, it means that within an element there is an internal deformation mode (with periodicity that is a multiple of the current unit cell size) along which the energy is decreasing. The search for this unstable direction is expedited by considering the phonon expansion, from which any displacement perturbation can be constructed, and identifying modes that are eigvenvectors of the linearized equations of motion with negative corresponding eigenvalues.

Suppose that a set of shifts $\bar{\boldsymbol{\delta}}$ minimize the SED (10) of an element for a given deformation gradient F. To determine if a larger basis would allow for a lower energy state to be reached, CCB views the current state as a high-symmetry configuration of the underlying infinite crystal. That is, if N_B' is any multiple of the current basis size, N_B, then the set of deformations describable by $\boldsymbol{\delta} \in \mathbb{R}^{N_B}$ is a subspace of those describable by $\boldsymbol{\gamma} \in \mathbb{R}^{N_B'}$. Thus, QC can consider the current shifts $\bar{\boldsymbol{\delta}}$ as a high-symmetry configuration on an appropriately defined energy surface for this larger space of shifts. A linear stability analysis is performed in order to determine the stability of each phonon mode (plane-wave normal modes of the crystal) that would break the high-symmetry state. If an unstable mode requiring a basis of size N_B' is identified, then it is energetically favorable to increase the basis size and work with shifts that belong to the space $\mathbb{R}^{N_B'}$.

Through the use of a block Fourier Transform each phonon mode can be checked independently and with computational effort only depending on the current basis size,

N_B, and the atomic potential cutoff. A full discussion and derivation of the three-dimensional phonon stability calculation is given by Elliott et. al. [12], here the pertinent details are outlined in the simplified one-dimensional context.

The starting point is the equations of motion for an infinite crystal whose current configuration is given by (9):

$$m_\alpha \frac{\partial^2}{\partial t^2}\left(x\begin{bmatrix}\ell_1\\ \alpha\end{bmatrix}\right) = -\sum_{\ell_2,\beta}\frac{\partial \phi_{\alpha\beta}}{\partial r}\left(x\begin{bmatrix}\ell_1\\ \alpha\end{bmatrix} - x\begin{bmatrix}\ell_2\\ \beta\end{bmatrix}\right). \tag{13}$$

In this section, sums over ℓ_j are from $-\infty$ to ∞ and sums over α and β are from 1 to N_B. The linearized equations of motion in terms of a perturbation $\mathbf{w}$ of the equilibrium configuration $\bar{\boldsymbol{\delta}}$ are

$$m_\alpha \frac{\partial^2}{\partial t^2}\left(w\begin{bmatrix}\ell_1\\ \alpha\end{bmatrix}\right) = -\sum_{\ell_2,\beta}\boldsymbol{\Phi}\begin{bmatrix}\ell_1 & \ell_2\\ \alpha & \beta\end{bmatrix} w\begin{bmatrix}\ell_2\\ \beta\end{bmatrix}, \tag{14}$$

where the tangent stiffness coefficients for the current model are given by

$$\begin{aligned}\boldsymbol{\Phi}\begin{bmatrix}\ell_1 & \ell_2\\ \alpha & \beta\end{bmatrix} = &-\frac{\partial^2\phi_{\alpha\beta}}{\partial r^2}\left(F(\ell_1-\ell_2)a + \bar{\delta}_\alpha - \bar{\delta}_\beta\right)\\ &+\sum_{\ell_3,\gamma}\frac{\partial^2\phi_{\alpha\gamma}}{\partial r^2}\left(F(\ell_1-\ell_3)a+\bar{\delta}_\alpha-\bar{\delta}_\gamma\right)\delta_{\ell_1\ell_2}\delta_{\alpha\beta}.\end{aligned} \tag{15}$$

In frequency space, the equations of motion become a collection of decoupled N_B by N_B linear systems as follows. The perturbation $\mathbf{w}$ is represented by plane-wave phonon modes as

$$w\begin{bmatrix}\ell\\ \alpha\end{bmatrix} = \int_{-\frac{1}{2}}^{\frac{1}{2}}\hat{w}(k,\alpha)e^{-2\pi i k\ell}\mathrm{d}k, \tag{16}$$

where $\hat{\mathbf{w}}$ is given by the discrete Fourier Transform,

$$\hat{w}(k,\alpha) = \sum_{\ell_1} w\begin{bmatrix}\ell_1\\ \alpha\end{bmatrix}e^{2\pi i k\ell_1} \qquad \text{for } k\in\left(-\frac{1}{2},\frac{1}{2}\right]. \tag{17}$$

Differentiating (17) twice, multiplying by the atomic masses m_α, and substituting (14), it is found that the amplitude of each phonon mode must satisfy

$$\begin{aligned}m_\alpha\frac{\partial^2\hat{w}}{\partial t^2}(k,\alpha) &= \sum_{\ell_1} m_\alpha\frac{\partial^2}{\partial t^2}\left(w\begin{bmatrix}\ell_1\\ \alpha\end{bmatrix}\right)e^{2\pi i k\ell_1}\\ &= -\sum_{\ell_1}\sum_{\ell_2,\beta}\boldsymbol{\Phi}\begin{bmatrix}\ell_1 & \ell_2\\ \alpha & \beta\end{bmatrix}w\begin{bmatrix}\ell_2\\ \beta\end{bmatrix}e^{2\pi i k\ell_1}.\end{aligned} \tag{18}$$

By the periodicity of the equilibrium configuration, $\bar{\boldsymbol{\delta}}$,

$$\boldsymbol{\Phi}\begin{bmatrix}\ell_1 & \ell_2\\ \alpha & \beta\end{bmatrix} = \boldsymbol{\Phi}\begin{bmatrix}0 & \ell_2-\ell_1\\ \alpha & \beta\end{bmatrix}. \tag{19}$$

Therefore, letting $\ell_3 = \ell_2 - \ell_1$ and exchanging the order of summation one obtains

$$\begin{aligned} m_\alpha \frac{\partial^2 \hat{w}}{\partial t^2}(k,\alpha) &= -\sum_{\ell_1} \sum_{\ell_3,\beta} \Phi \begin{bmatrix} 0 & \ell_3 \\ \alpha & \beta \end{bmatrix} w \begin{bmatrix} \ell_3 + \ell_1 \\ \beta \end{bmatrix} e^{2\pi i k \ell_1} \\ &= -\sum_{\ell_3,\beta} \Phi \begin{bmatrix} 0 & \ell_3 \\ \alpha & \beta \end{bmatrix} e^{-2\pi i k \ell_3} \sum_{\ell_1} w \begin{bmatrix} \ell_3 + \ell_1 \\ \beta \end{bmatrix} e^{2\pi i k (\ell_3 + \ell_1)} \\ &= -\sum_{\ell_3,\beta} \hat{w}(k,\beta) \Phi \begin{bmatrix} 0 & \ell_3 \\ \alpha & \beta \end{bmatrix} e^{-2\pi i k \ell_3}, \end{aligned} \tag{20}$$

where the last equality follows by noting that as ℓ_1 ranges over all lattice sites so does $\ell_3 + \ell_1$. Thus, the inner sum is precisely the discrete Fourier Transform (17) of the perturbation.

Finally, the block-diagonalized linearized equations of motion about the equilibrium configuration are given in frequency space as

$$m_\alpha \frac{\partial^2 \hat{w}}{\partial t^2}(k,\alpha) = -\sum_{\beta} K_{\alpha\beta}(k) \hat{w}(k,\beta) \qquad \text{for every } k \in \left(-\frac{1}{2}, \frac{1}{2}\right]. \tag{21}$$

The dynamical matrix $\mathbf{K}(k) = \left[K_{\alpha\beta}(k)\right]$ is given by

$$K_{\alpha\beta}(k) = \sum_{\ell_3} \Phi \begin{bmatrix} 0 & \ell_3 \\ \alpha & \beta \end{bmatrix} e^{-2\pi i k \ell_3}. \tag{22}$$

Recall that solutions of a linear system of second-order differential equations, such as (21), are bounded for all time provided that all eigenvalues of $\mathbf{K}(k)$ are positive. The same holds for solutions to (14) in the energy norm when all eigenvalues are positive for every k. Note that the tangent stiffness coefficients of the linearized equations of motion (14) are symmetric and thus have real eigenvalues. So, all eigenvalues of $\mathbf{K}(k)$ must also be real since the eigenvalues are invariant under Fourier transformation.

By the Hamiltonian formulation of (14), the Hamiltonian energy

$$\frac{1}{2} \sum_{\ell_1,\alpha} m_\alpha \left(\frac{\partial w}{\partial t} \begin{bmatrix} \ell_1 \\ \alpha \end{bmatrix} \right)^2 + \frac{1}{2} \sum_{\ell_1,\alpha} \sum_{\ell_2,\beta} \Phi \begin{bmatrix} \ell_1 & \ell_2 \\ \alpha & \beta \end{bmatrix} w \begin{bmatrix} \ell_1 \\ \alpha \end{bmatrix} w \begin{bmatrix} \ell_2 \\ \beta \end{bmatrix} = E \tag{23}$$

is constant for any dynamical solution $\mathbf{w}(t)$. The steady solution of (14), $\mathbf{w} = 0$, is thus stable if the linearized potential energy $V(\mathbf{w})$ is positive definite, that is, if

$$V(\mathbf{w}) = \sum_{\ell_1,\alpha} \sum_{\ell_2,\beta} \Phi \begin{bmatrix} \ell_1 & \ell_2 \\ \alpha & \beta \end{bmatrix} w \begin{bmatrix} \ell_1 \\ \alpha \end{bmatrix} w \begin{bmatrix} \ell_2 \\ \beta \end{bmatrix} > 0 \tag{24}$$

for every $\mathbf{w}$ that is not a constant translation. By Parseval's theorem,

$$V(\mathbf{w}) = \sum_{\alpha,\beta} \int_{-\frac{1}{2}}^{\frac{1}{2}} K_{\alpha\beta}(k) \hat{w}(k,\alpha) \overline{\hat{w}(k,\beta)} \, \mathrm{d}k, \tag{25}$$

so we conclude that solutions are stable if for every k, all eigenvalues of $\mathbf{K}(k)$ are positive except for the translation mode at $k = 0$.

3.2 Cascading Cauchy-Born algorithm

In principle, to ensure the phonon stability, and therefore local energy minimization, of a QC continuum element's underlying crystal structure, it would be necessary to check all possible basis sizes by checking every k. However, it is noted that eigenvalues of the dynamical matrix $\mathbf{K}(k)$ vary continuously with k. This implies that if one mode becomes unstable then its neighboring modes (in k-space) will also become unstable. Thus, it will be enough to sample the phonon mode eigenvalues at a finite number of k-points and rely on the mentioned continuity to ensure that an acceptable tolerance is reached for the identification of instabilities.

The CCB algorithm is invoked at the end of each QC load step once a local energy minimum for the current set of basis sizes[4] has been identified. One parameter, M_B, is required to set the maximum allowed number of atoms in an element's CB basis. The algorithm is formulated so that at any stage during the simulation each element's underlying periodic structure can be described with a basis containing M_B atoms. To be explicit, the CCB algorithm used here is given, in pseudocode, as:

```
1 for every element e
2   set ℓ = M_B/N_B^e
3   for j = 1, ..., floor(ℓ/2)
4     compute λ_1, the smallest eigenvalue of K(j/ℓ; F^e, δ^e)
5     if λ_1 ≤ 0
6         set N_B^e = N_B^e · ℓ/gcd(j, ℓ) and proceed to next element
7 if any elements increased their basis size
8   minimize energy with the new representation and goto 1
```

In the above, superscript e refers to element number, floor$(\cdot)$ is the greatest integer function, and gcd$(\cdot,\cdot)$ is the greatest common divisor function. Here we explicitly indicate the dependence of $\mathbf{K}$ on the deformation gradient and shift in the element. This dependence comes through Φ as shown in (15). For each element, line 2 determines the maximum allowable period increase ℓ that can occur and still result in a periodic structure that is describable with an M_B atom basis. Lines 3 to 6 then check the stability of the phonon mode with wavenumber j/ℓ and if an instability is identified the current basis size of the element N_B^e is updated to its new value by multiplying the previous value by the appropriate period increase.[5] If any instabilities are identified and an element's basis size changes as a result, the updated QC potential energy must be re-minimized and the CCB process performed for the new energy minimizing configuration. In this way, it is possible for an element's basis size to cascade from its initial value to a final larger value that guarantees that the energy can not be reduced further by an additional basis increase.

For the CCB algorithm defined above to work as intended, some care must be taken to choose the parameter M_B appropriately. In particular, M_B must be a multiple of the reference essential basis size N_B^o. Further, since small period increases are the most commonly observed type of phase transformations in real materials, it seems reasonable to make sure that M_B has a number of repeated small integer factors. For instance, we suggest $M_B = 2^2 \cdot 3^2 \cdot 5 \cdot N_B^o = 180 N_B^o$ which allows for all possible period increases up to an increase of 6 as well as certain larger period increases including $9, 10, 12, 15, 18,$

[4] Each finite element e has its own current basis size N_B^e. Here we refer to the set of basis sizes of all elements in the mesh.

[5] Only positive wave numbers between 0 and $\frac{1}{2}$ are tested, since $\lambda_1(-k) = \lambda_1(k)$.

and 20. A minimum value of $M_B = 2^3 \cdot 3^2 \cdot 5 \cdot 7 \cdot N_B^o = 2520 N_B^o$ is required if all period increases up to a value of 10 are to be considered. These are large numbers, but we point out that such large bases would not be expected to occur aside from cases of failure or amorphization where CCB would react by increasing basis size to M_B. CCB shows its main power by sampling the possibly quite large basis size M_B, but only using a minimum of degrees of freedom during expensive minimization computations. The following section describes the circumstances in which the CCB algorithm will agree exactly with a simulation using the full M_B degrees of freedom within each element.

3.3 Analysis of the CCB algorithm

To assess the accuracy of the CCB algorithm and the conditions under which it is applicable, it is first necessary to classify the types of phase transformations represented by lattice instabilities. The CCB algorithm is applied to the infinite lattice underlying a continuum finite element. In 1D, this lattice is a uniformly strained infinite chain of atoms with no external forces and a periodic deformation associated with the shifts that is commensurate with the maximum basis size M_B. Since the algorithm is applied after a full QC relaxation, all atoms in the chain satisfy force equilibrium, i.e.,

$$\sum_{\ell_2,\beta} \frac{\partial \phi_{\alpha\beta}}{\partial r} \left(x \begin{bmatrix} \ell_1 \\ \alpha \end{bmatrix} - x \begin{bmatrix} \ell_2 \\ \beta \end{bmatrix} \right) = 0 \qquad \text{for all } \ell_1, \alpha, \tag{26}$$

where initially, $\mathbf{x}$ is of the form (9). Minimizing out the shifts as in (11) gives $\boldsymbol{\delta}(F)$ for the current deformation gradient. Let $\mathbf{w}$ be a M_B-periodic perturbation of the current state, then the internal force, f, at the perturbed state is

$$\begin{aligned} f(\mathbf{w}, F) \begin{bmatrix} \ell_1 \\ \alpha \end{bmatrix} = - \sum_{\ell_2=-\infty}^{\infty} \sum_{\beta} \frac{\partial \phi_{\alpha\beta}}{\partial r} \Bigg(& F(\ell_1 - \ell_2) a + \delta_\alpha(F) + w \begin{bmatrix} \ell_1 \\ \alpha \end{bmatrix} \\ & - \delta_\beta(F) - w \begin{bmatrix} \ell_2 \\ \beta \end{bmatrix} \Bigg) \end{aligned} \tag{27}$$

for all $\ell_1 = 1, \ldots, M_B/N_B$ and $\alpha = 1, \ldots, N_B$.

Since f is a continuously differentiable function of all its parameters, the implicit function theorem says that at any point $(\mathbf{w}_0, F_0)$ where $\nabla_{\mathbf{w}} f$ is nonsingular there is a unique function $\mathbf{w}(F)$ defined in some small region about $(\mathbf{w}_0, F_0)$ that satisfies the implicit equation

$$f(\mathbf{w}(F), F) = 0. \tag{28}$$

Loss of stability of the current high-symmetry state occurs precisely when one or more eigenvalues of $\nabla_{\mathbf{w}} f$ become negative. At these points, many things can occur. Here a discussion of the case when a single eigenvalue becomes zero and another solution branch crosses creating a bifurcation point is presented. The precise nature of how this second solution crosses determines the physics of the loss of stability. Fig. 2 gives a schematic of the most common types of bifurcation. Subcritical bifurcations correspond to first-order transitions, and the crossing solutions are unstable in all sufficiently small neighborhoods of the current solution. Thus, the stable portions of the bifurcating branches are located far away from the bifurcation point which causes the discontinuous change associated with a first-order transition. Supercritical and transcritical bifurcations result in second-order transitions. Stable sections of the crossing solutions extend

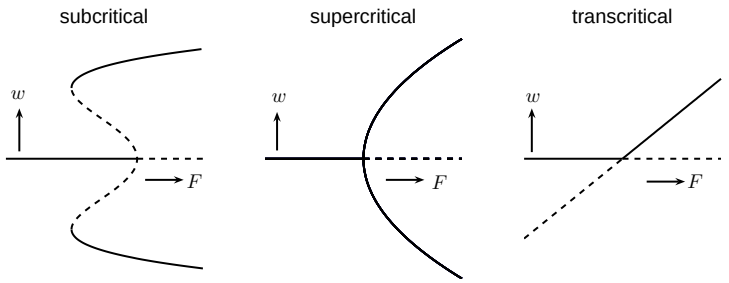

Fig. 2 Simple mode subcritical, supercritical, and transcritical bifurcations at a crossing from stable (solid line) to unstable (dashed line) equilibrium solutions. Subcritical bifurcations correspond to first-order transitions, in which the positions for the stable solution are not continuous as a function of the loading parameters. In supercritical and transcritical bifurcations, the branches emanating from the stable solution are themselves stable for increasing F.

forward in the positive loading parameter direction from the current solution. Thus, the stable solution continuously transitions from one branch to another.

Having defined the types of instabilities that commonly occur, we now turn to an analysis of the CCB algorithm. Consider a continuum element currently having a basis of size N_B. The behavior of the CCB algorithm will be compared to the case of simply using M_B atoms for the basis. In this case the energy minimization step occurs with respect to an M_B-dimensional energy landscape defined by $W(F,\boldsymbol{\gamma})$ for $\boldsymbol{\gamma} \in \mathbb{R}^{M_B}$. For the smaller basis, the motion is restricted to the subspace V corresponding to deformations describable by $\boldsymbol{\delta} \in \mathbb{R}^{N_B}$.

Due to the nature of the QC incremental-loading process there is little chance of ever finding the exact deformation gradient at which a phonon eigenvalue is zero. The more likely situation is that successive increments to the loading-parameter will result in equilibrium configurations that straddle the corresponding bifurcation point. One of these configurations will be stable and the other unstable. The unstable configuration is a local minimum with respect to V, however it is a saddle point with respect to the full energy landscape on the larger space $\mathbb{R}^{M_B}$. Assuming that the step-size is sufficiently small and that the QC model has no degeneracies, then this first instability will correspond to a single set of phonon modes ($\pm k$) that have become unstable before any others.

Suppose this first instability corresponds to a second-order phase transformation. After increasing the basis to accommodate the new mode, the relaxation will be proportional to the square-root of the load step. Since the energy surface is continuous, the stability with respect to all other phonon modes at the saddle point implies their stability in a neighborhood and therefore, all other phonon modes remain stable at the new minimum. Thus, the CCB algorithm will find the same local minimum that the element that started with the larger basis size does.

The situation is less clear for a first-order phase transformation. In this case a large relaxation will occur regardless of the loading-step size. During this relaxation, it is conceivable that additional symmetry breaking motions occurring in the higher dimensional system would be energetically favorable. The CCB algorithm may not be able to identify these. Thus, the energy minimizers found by an element using CCB and an element with the fixed larger basis of size M_B might be very far apart.

First-order phase transformations often result in novel material properties and are an important part of the behavior of many advanced materials. Thus, the authors are actively investigating this and other issues surrounding the use of CCB kinematics for the study these materials.

4 A one-dimensional example of period extensions

As an example of a physical system where CCB kinematics are required to obtain accurate results with minimal computational effort, consider a one-dimensional bi-atomic crystal with long-range Lennard-Jones (LJ) pair interactions. Three LJ potentials are required to describe the atomic interactions: (i) interaction between two 'a' atoms $\phi_{aa}(r)$, (ii) interactions between two 'b' atoms $\phi_{bb}(r)$, and (iii) interactions between an 'a' atom and a 'b' atom $\phi_{ab}(r)$. The LJ pair-potential is given by[6]

$$\varphi(r) = 4\varepsilon \left[\left(\frac{\sigma}{r}\right)^{12} - \left(\frac{\sigma}{r}\right)^{6} \right], \tag{29}$$

and the interaction parameters are: $\varepsilon_{aa} = 1.0, \sigma_{aa} = 1.0$, $\varepsilon_{bb} = 1.0, \sigma_{bb} = 0.85$, and $\varepsilon_{ab} = 0.1, \sigma_{ab} = 0.475$. These parameters create a potential in which all atoms are equally spaced in the reference configuration, but for positive strain b atom pairs clump together, requiring a larger basis to describe the structure. The parameters were chosen based on the intuition that a atoms would provide a strong, evenly spaced underlying lattice, whereas under load b atoms would form a more closely packed lattice leading to a larger periodicity than the essential reference basis.

Here, a smooth cutoff is applied by choosing a radius r_{cut}, and letting

$$\phi(r) = \begin{cases} \varphi(r) + Ar^2 + B, & |r| \le r_{cut}, \\ 0, & |r| > r_{cut}, \end{cases} \tag{30}$$

where

$$\begin{aligned} A &= -\frac{1}{2r_{cut}} \frac{\partial \varphi}{\partial r}(r_{cut}), \\ B &= \frac{r_{cut}}{2} \frac{\partial \varphi}{\partial r}(r_{cut}) - \varphi(r_{cut}). \end{aligned} \tag{31}$$

This ensures that $\phi(r) = 0$ for any $|r| \ge r_{cut}$, and that ϕ has continuous first derivative at $|r| = r_{cut}$. For the computations below a value of $r_{cut} = 2.0$ has been used which gives a third-neighbor cutoff in the reference configuration.

4.1 Behavior of the uniformly strained crystal

The unloaded reference configuration for the 1D crystal can be described by an essential basis that contains two atoms, one of each type. Each atom is symmetrically positioned between its nearest neighbors, which are of opposite species. This configuration is schematically illustrated in Fig. 3(b). To gain an understanding of how this material model behaves, a bifurcation diagram is generated using the technique of Elliott [15] which is further described in another article in the current issue and in Elliott et al. [13].

[6] Here, subscripts indicating the type of species interaction, e.g. aa, bb, or ab, are suppressed.

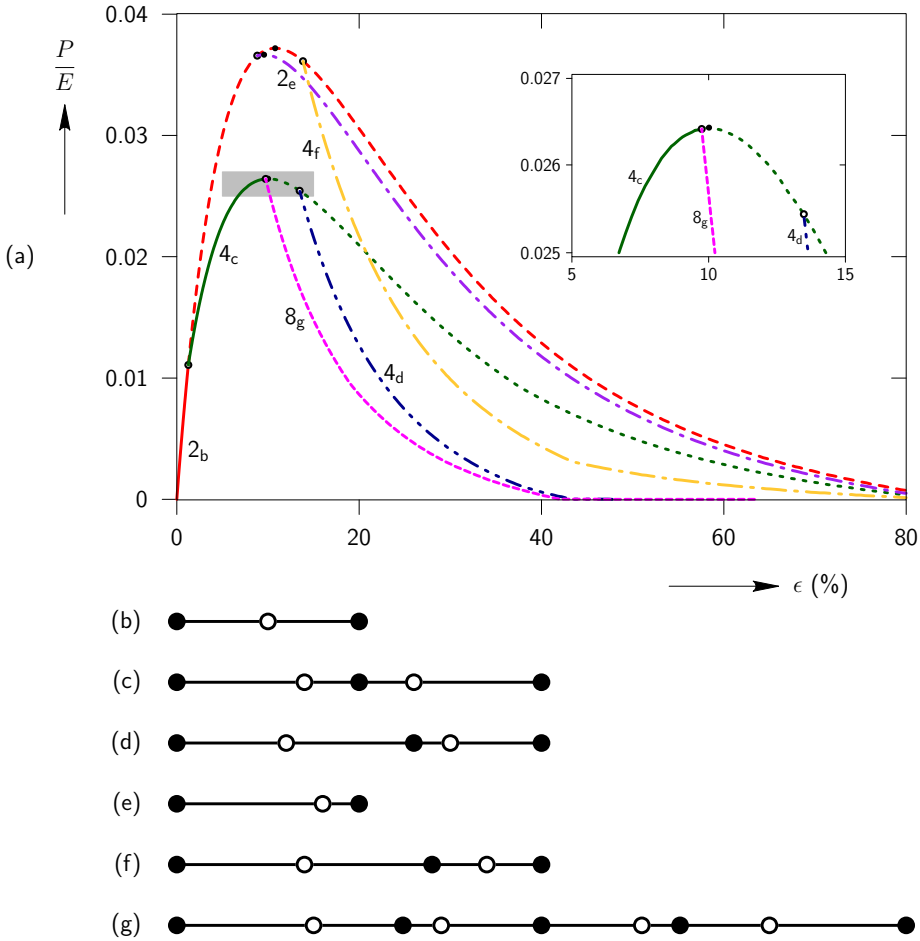

Fig. 3 Normalized force vs. strain behavior for the bi-atomic one-dimensional crystal. Equilibrium paths are labeled with the number of atoms in the corresponding unit cell and a subscript that refers to the sub-figure that illustrates the symmetry of the arrangement of atoms within the equilibrium unit cell. (a) Bifurcation diagram showing the two stable path segments corresponding to a 2-lattice configuration, 2_b, and a 4-lattice configuration, 4_c. The schematics in (b)–(g) indicate the symmetry of the equilibrium paths in (a) with the corresponding subscript label. Paths 2_b, 4_c and 8_g have mirror symmetry within the unit cell.

Equilibrium paths for various lattice periodicities are computed as the uniform strain is varied and the normalized conjugate force P for each configuration is computed. Fig. 3(a) displays the resulting force-strain behavior. The conjugate force is defined by

$$P = \frac{\partial \widetilde{W}}{\partial F}, \tag{32}$$

and the strain is $\epsilon = F - 1$. P is normalized by the reference Young's modulus $E = \left.\frac{\partial^2 \widetilde{W}}{\partial F^2}\right|_{F=0}$. For the current model this modulus is found to be $E = 122.28\varepsilon_{aa}$ where ε_{aa} is used only to provide consistent units. The solid line segment connected

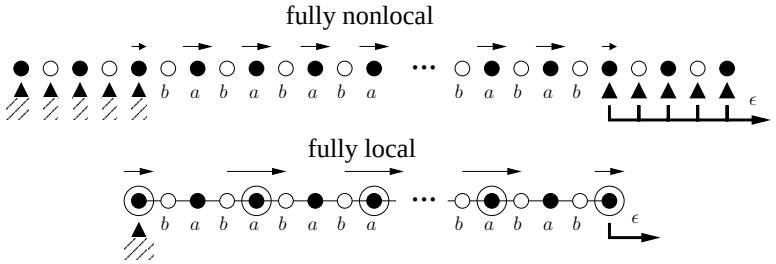

Fig. 4 Schematic diagram showing the chain of atoms and the distributed forces applied to it for both the fully-nonlocal and fully-local cases. In addition to the distributed load, the chain is held on the left side and uniformly strained to the right. The chain consists of alternating 'a' and 'b' atoms. The forces are applied only to 'a' atoms. This can be thought of as a body-force loading, such as that due to the affect of an external field that interacts only with the 'a' atoms. In the nonlocal case, the external forces on the end atoms are halved for consistency between the models. The forces in the local model are integrated to the nodes according to (37).

to the origin in Fig. 3(a) is the primary equilibrium path that the crystal follows upon initial extension. This path corresponds to a 2-lattice structure (see Fig. 3(b)) and is stable until a supercritical bifurcation point is encountered near $\epsilon = 1.25\%$. For larger strains the force along this path continues to increase but the configuration is now unstable. The first bifurcation is a translation-symmetry breaking bifurcation and the emerging equilibrium path (4_c) has a 4-lattice structure as indicated in Fig. 3(c). For strains between $\epsilon = 1.25\%$ and $\epsilon = 9.75\%$ this 4-lattice configuration is the only stable structure, and no stable structures exist for higher strains, indicating that the crystal fractures at a strain of $\epsilon = 9.75\%$. This failure occurs via an 8-lattice deformation mode that corresponds to the unstable equilibrium path 8_g in Fig. 3(a). If this 8-lattice failure mode had not occurred, the 4-lattice equilibrium path 4_c would have become unstable at the turning-point or limit-load located just to the right, in Fig. 3(a), at $\epsilon = 10.01\%$. An instability of this type corresponds to a long wavelength continuum-scale deformation mode where the Young's modulus goes to zero. In the current 1D setting such an instability is indicative of fracture, but in the more general 3D setting turning-points of this type lead to shear-band-like behavior which ultimately results in the formation of dislocations in the crystal. This type of behavior has been extensively studied by researchers such as Yip et. al. [16]. In addition to the two equilibrium paths with stable segments (2_b and 4_c) other equilibrium paths exist in Fig. 3(a), but they are always unstable. The number of atoms in the basis and the symmetry of their arrangement in the unit cell for each path in Fig. 3(a) can be found in Fig. 3(b)–(g).

Thus, the crystal's behavior may correctly be described with a 2-lattice CB kinematics up to the bifurcation at $\epsilon = 1.25\%$, at which point the CCB technique will detect the instability, identify the 4-lattice kinematics as the new physically relevant description, and switch to the appropriate 4-lattice CB kinematics. Similarly at a strain of $\epsilon = 9.75\%$ CCB will detect the instability leading to the 8-lattice and the failure of the crystal. In this way the period-doubling phase transformations that occur in this material model are correctly captured—a behavior that a fixed CB kinematics technique utterly misses, as shown in the next subsection.

4.2 Approximating the response of a non-uniformly deformed chain

The main purpose of the QC method is to accurately approximate atomistic BVPs where non-uniform deformations occur and to do this with a minimum of computational effort. Without CCB kinematics the QC method must use a full atomistic description to accurately solve problems where phase transformations that increase the unit cell occur. In this section the response of a chain of atoms subjected to a distributed uniform external loading is studied. A schematic diagram of the chain and applied loading is showin in Fig. 4. This applied loading will result in a non-uniform deformation, a phase transformation that propagates through the chain, and finally fracture at a stress concentration. Several fully-local simulations using CCB at various levels of mesh refinement along with a fully-refined local simulation not using CCB are compared to a fully-nonlocal simulation to illustrate the importance of CCB in this case. The fully-nonlocal simulation is identical to a fully-atomistic simulation and therefore serves as the exact result that local QC attempts to accurately reproduce using as few local repsites as possible. The terms nonlocal and atomistic are used interchangeably in what follows.

A chain of 2048 atoms, alternating between 'a' and 'b' types is simulated. To avoid surface relaxation of the fully-atomistic chain and resulting premature fracture, extra atoms on each end of the chain will contribute boundary conditions as described below. Therefore, a chain with 1028 nonlocal repsites with basis size $N_B^0 = 2$ is created, and initial positions are set to be $X^i = (i-3)a_0$. Only the energy of the original 2048 atoms is computed, giving

$$\mathit{\Pi}(\mathbf{u}, \boldsymbol{\delta}) = \sum_{i=3}^{1026} \left[\sum_{\alpha=1}^{2} E_\alpha^i(\mathbf{u}, \boldsymbol{\delta}) - f^i u^i \right], \tag{33}$$

where the third-neighbor energy is

$$E_\alpha^i(\mathbf{u}, \boldsymbol{\delta}) = \frac{1}{2} \sum_{j=-2}^{2} \sum_{\beta=1}^{2} \phi(X^{i+j} + u^{i+j} + \delta_\beta^{i+j} - X^i - u^i - \delta_\alpha^i). \tag{34}$$

The extra two unit cells are precisely what is needed to ensure that each of the interior 2048 atoms has all six closest neighbors. The reference configuration for the chain is taken to be that of equal atomic spacing, as in Fig. 3(b). The applied forces f^i are given by

$$f^i = \begin{cases} \frac{\varepsilon_{aa}}{1024\sigma_{aa}}, & i = 4, \ldots, 1026, \\ \frac{\varepsilon_{aa}}{2048\sigma_{aa}}, & i = 3 \text{ or } 1027, \\ 0, & \text{otherwise.} \end{cases} \tag{35}$$

The loading proceeds through a series of steps increasing the overall nominal strain ϵ, i.e., the change in length from the reference configuration divided by the reference length. The nominal strain is increased from ϵ to ϵ' by multiplying all atom positions of the current configuration by $\frac{\epsilon'}{\epsilon}$. After stretching, the inner 2048 degrees of freedom are relaxed by minimizing the energy of (33) with respect to u^i for $i = 4, \ldots, 1026$ and δ_2^i for $i = 3, \ldots, 1026$.

The formulation for the local chain is simpler since surface relaxation cannot occur. Refinement is facilitated by choosing 2^n finite elements for $0 \leq n \leq 10$, which corresponds to choosing $2^n + 1$ local repsites. All elements have $N_B^0 = 2$, and $M_B = \frac{1024}{2^n}$.

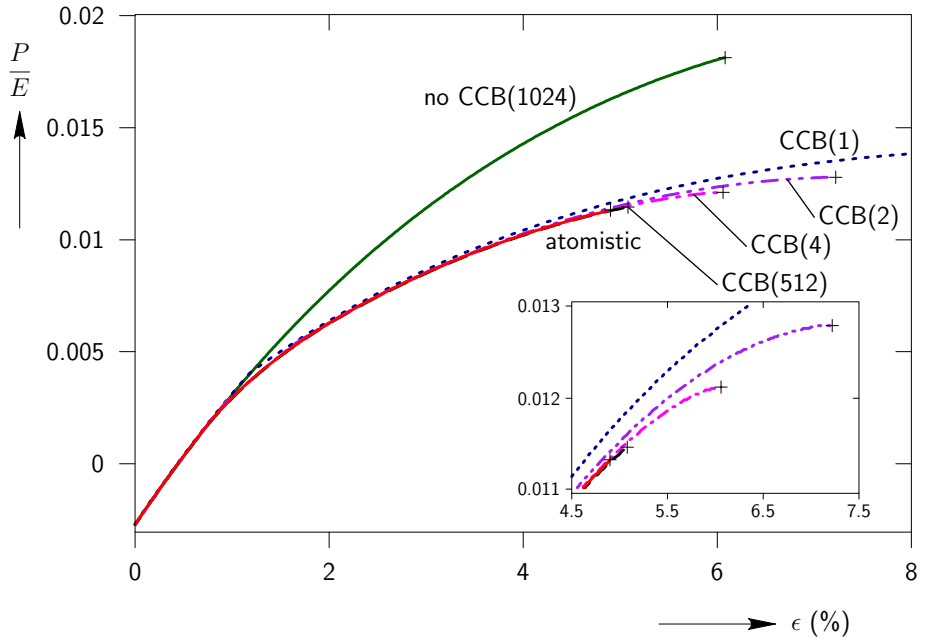

Fig. 5 Normalized conjugate force vs. nominal strain for a chain with applied external forces as described in text. Here the numbers in parentheses indicate the number of QC finite elements used for the corresponding curve. Failure points are indicated by + signs.

The initial positions are $X^i = a_0(i-1)\frac{1024}{2^n}$, and the potential energy is

$$\tilde{I\!I}(\mathbf{u}) = \sum_{i=1}^{2^n} \left[a_0 \frac{1024}{2^n} \widetilde{W}\left(\frac{u^{i+1} - u^i}{X^{i+1} - X^i} \right) - \tilde{f}^i u^i \right], \tag{36}$$

where $\widetilde{W}$ is as in (12) and the forces of the nonlocal simulation are integrated to the local repsites giving

$$\tilde{f}^i = \begin{cases} \frac{\varepsilon_{aa}}{2^n \sigma_{aa}} & i = 2, \ldots, 2^n, \\ \frac{\varepsilon_{aa}}{2^{n+1} \sigma_{aa}} & i = 1 \text{ or } 2^n + 1. \end{cases} \tag{37}$$

The load steps work as in the nonlocal simulation, with an overall nominal strain being applied before minimizing the energy (36) with respect to the internal repsite displacements u^i for $i = 2, \ldots, 1023$. The local and nonlocal simulations are consistent in the sense that for any uniform deformation, all simulations assign the same energy to the chain.

The force-strain response of the nonlocal and local calculations is presented in Fig. 5, where the conjugate force P plotted in the figure is defined as

$$P = \frac{1}{1024 a_0} \frac{\partial \tilde{I\!I}}{\partial \epsilon}, \tag{38}$$

where $\tilde{I\!I}$ is replaced by $I\!I$ for the nonlocal case. Fig. 5 shows the results for local QC models with 1, 2, 4, and 512 elements with CCB kinematics and a 1024 element model

without CCB, compared with the exact atomistic result. The atomistic curve shows a discontinuity in slope at a nominal strain of $\epsilon = 0.69\%$ when a phase transformation to a 4-lattice structure is initiated at the left end of the chain. This is discussed in more detail below. The strain increases until fracture occurs in the chain at a nominal strain of $\epsilon = 4.92\%$. The 1024 element model cannot undergo phase transformations and therefore once the exact solution transforms, there is a large error in its conjugate force. There is also a large error in the failure point predicted by this model since fracture occurs through a 2-lattice path as in Fig. 3(e) rather than through a lower symmetry path as in the 8-lattice case of Fig. 3(g). In contrast, all of the other local QC simulations with CCB show much smaller errors before fracture and increasing accuracy in approximating the fracture point with refinement.

The reduction in errors of the CCB models is demonstrated more clearly in Fig. 6(a) that shows a plot of the normalized error in the conjugate force for the range of strains where phase transformations occur. The sudden discontinuities in slope of the CCB curves correspond to period doubling events that occur within one of the elements of the mesh. The magnitude of the error is reduced with increasing refinement up to a model containing 4 elements and then increases somewhat. This increase is due to the nonuniform deformation that leads to a difference between a fully-refined local QC simulation that contains all lattice sites as local repsites and a fully-atomistic simulation, regardless of the basis size within the elements. Although a local QC simulation will converge to a well-defined solution as the number of local repsites is increased, this solution is generally *not* the exact solution.

Fig. 6(b) shows progress of the phase transformation as a percent of the chain length that is in the 4-lattice state. The atoms in the fully-nonlocal (atomistic) simulation remain in their 2-lattice phase until the nominal strain reaches a value of $\epsilon = 0.69\%$. At this point the phase transformation from the 2-lattice to the 4-lattice structure described Section 4.1 is initiated at the left end of the chain, where the cumulative effects of the distributed external load are the strongest. As the nominal strain is increased from this critical value of $\epsilon = 0.69\%$ to a value of $\epsilon = 2.7\%$ the transformed region of the chain grows from the left until the entire chain has transformed to the 4-lattice structure. Beyond this point the chain continues to deform and remains in the 4-lattice structure. The local QC CCB models track this behavior in a discontinuous fashion dictated by the level of refinement of the mesh used. The most refined model with 512 elements follows the atomistic curve almost exactly.

These results clearly demonstrate the need for obtaining an appropriate basis size in order to get an accurate approximation of the material properties. The choice of proper basis size outweighs the importance of refinement in determining conjugate force prior to fracture, and the CCB algorithm provides an efficient way of finding a minimal basis size that describes the desired behavior.

5 Future work

This paper presents a multilattice QC formulation based on the new idea of Cascading Cauchy-Born (CCB) kinematics. In this approach, a phonon stability analysis is carried out within each finite element in the continuum region at the end of every load step to detect energetically favorable period extensions in the unit cell used for CB calculations. This is necessary in order to allow for certain phase transformations to occur. The method is applied to two 1D test cases: a uniformly strained infinite crystal and a

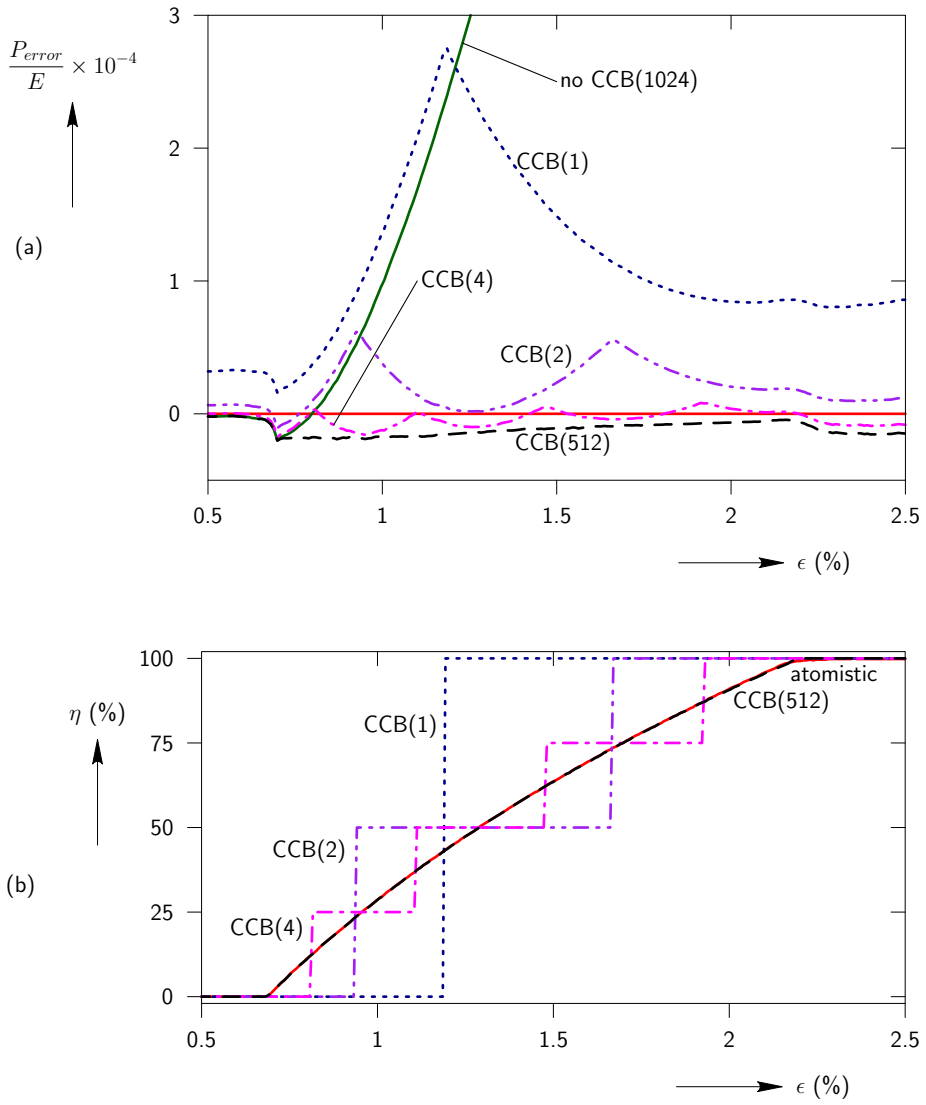

Fig. 6 (a) Normalized error in the conjugate force vs. nominal strain. P_{error} is defined as the difference between the conjugate force calculated in a given simulation and the exact value obtained from the nonlocal simulation. (b) Phase fraction η (in percent) of the chain that is in the period-doubled phase. Here the numbers in parentheses indicate the number of QC finite elements used for the corresponding curve.

finite-sized crystal experiencing a non-uniform deformation. In both cases it is shown that the use of CCB kinematics is critical for obtaining the correct behavior, which includes phase transformations involving period doubling and period quadrupling.

Multilattice QC is in its initial stages of development and a number of issues remain that must be addressed. Perhaps most straightforward is the extension to three

dimensions (3D). The phonon stability analysis that lies at the heart of CCB can readily be generalized to 3D. In fact, in the past it has been applied only to 3D problems [12,13], so that the implementation used here constitutes a simplified special case. The computational advantages are amplified in higher dimensions, e.g., just checking period doubling in each direction and their combinations allows one to sample a unit cell with 8 times the number of atoms. However, additional work is needed on the identification of the non-essential unit cell associated with an unstable 3D mode, the handling of simultaneously unstable symmetry-related modes, and the development of efficient techniques for sampling of k-points.

A more fundamental issue is related to the correct treatment of first-order transformations using this approach. This is an important issue since many key phase transformations are first-order in nature. CCB kinematics will work in this case in the sense that the algorithm will provide a definite result. However, it is unclear at this point whether this would be the "correct" result, or even if it is possible to state what the correct result is when an energy minimization scheme is used to study a problem that may be inherently dynamic. We plan to explore this issue further by applying CCB kinematics to situations where first-order transformations occur and analyzing the resulting behavior.

Another important issue is that CB kinematics for multilattices can have energetically equivalent variants with identical elastic properties. Note that this can occur even when CCB kinematics are not used. A simple example is dimerization in a two atom unit cell, which can occur to the "left" or the "right" (in a 1D setting). (See Fig. 3(e) for an example of dimerization.) At a continuum level these two variants are indistinguishable and therefore the degeneracy in the internal structure is irrelevant. However, since in QC local continuum regions can transform into nonlocal atomistic regions, adjoining finite elements with different degenerate structures will introduce spurious anti-phase boundaries into the system. A possible solution to this problem is the incorporation of interfacial energy between finite elements similar to cohesive-zone formulations. This approach has the additional benefit of providing a lengthscale to any resulting microstructure in the continuum region. Preliminary work along these lines is reported in [17].

Finally, there are a number of issues related specifically to the application of QC to multilattices, such as the correct way to address so-called "ghost forces" [2] in this case. For simple lattices this concept is well-defined and efficient as shown recently [14]. However, for multilattices this will have to be revisited. Another example relates to the implementation of mesh adaption in the light of CCB kinematics. In particular, period increase should be prevented if it would cause the new multilattice basis to contain more atoms than is appropriate for the size of the element. In this case, the identification of an instability should cause the atomistic structure contained within the element to be fully-refined and converted to an atomistic region.

These are just some of the issues that are actively being investigated with an eye toward applications to phase transforming materials, such as quartz and shape memory alloys, undergoing fracture and other failure events.

Acknowledgements This work was supported in part by the Department of Energy under Award Number DE-FG02-05ER25706, NSF grant DMS-0304326, and by the University of Minnesota Supercomputing Institute.

References

1. E. B. Tadmor, M. Ortiz and R. Phillips, "Quasicontinuum Analysis of Defects in Solids", *Phil. Mag. A*, **73**, 1529-1563 (1996).
2. V. B. Shenoy, R. Miller, E. B. Tadmor, D. Rodney, R. Phillips and M. Ortiz, "An Adaptive Finite Element Approach to Atomic-Scale Mechanics : The Quasicontinuum Method", *J. Mech. Phys. Solids*, **47**, 611-642 (1999).
3. R. E. Miller and E. B. Tadmor, "The Quasicontinuum Method: Overview, Applications and Current Directions", *J. Computer-Aided Materials Design*, **9**, 203-239 (2002).
4. M. Born and K. Huang, *Dynamical Theory of Crystal Lattices*, Clarendon Press, Oxford, 1954.
5. M. Pitteri, "On the Kinematics of Mechanical Twinning in Crystals", *Arch. Rat. Mech. Anal.*, **88**, 25-57 (1985).
6. G. Zanzotto, "Twinning in Minerals and Metals: Remarks on the Comparison of a Thermoelastic Theory with some Available Experimental Results: Notes I and II", *Atti Accademia Nazionale dei Lincei, Rend. Fis.*, **82**, 725742 and 743756 (1988).
7. E. B. Tadmor, G. S. Smith, N. Bernstein and E. Kaxiras, "Mixed Finite Element and Atomistic Formulation for Complex Crystals", *Phys. Rev. B*, **59**, 235-245 (1999).
8. G. S. Smith, E. B. Tadmor and E. Kaxiras, "Multiscale Simulation of Loading and Electrical Resistance in Silicon Nanoindentation", *Phys. Rev. Lett.*, **84**, 1260-1263 (2000).
9. E. B. Tadmor, U. V. Waghmare, G. S. Smith and E. Kaxiras, "Polarization Switching in $PbTiO_3$: An ab initio Finite Element Simulation", *Acta Mater.*, **50**, 2989-3002 (2002).
10. G. Zanzotto, "On the Material Symmetry Group of Elastic Crystals and the Born Rule", *Arch. Rational Mech. Anal.*, **121**, 1-36 (1992).
11. G. Zanzotto, "The Cauchy-Born Hypothesis, Nonlinear Elasticity and Mechanical Twinning in Crystals", *Acta Cryst.*, **A52**, 839-849 (1996).
12. R. S. Elliott, N. Triantafyllidis and J. A. Shaw, "Stability of Crystalline Solids – I: Continuum and Atomic Lattice Considerations", *J. Mech. Phys. Solids*, **54**, 161-192 (2006).
13. R. S. Elliott, J. A. Shaw and N. Triantafyllidis, "Stability of Crystalline Solids – II: Application to Temperature-Induced Martensitic Phase Transformations in a Bi-Atomic Crystal", *J. Mech. Phys. Solids*, **54**, 193-232 (2006).
14. M. Dobson and M. Luskin, "Analysis of a Force-Based Quasicontinuum Approximation", *arXiv:math.NA/0611543*, 2006.
15. R. S. Elliott, "Multiscale Bifurcation and Stability of Multilattices", *J. Comput-Aid. Mat. Des.*, submitted, (2007).
16. S. Yip, J. Li, and T. Zhu, "Atomistic Measures of Strength, Deformation and Reactivity: Toward Multiscale Modeling of Chemo-Mechanical Phenomena", Proceedings of the Third International Conference on Multiscale Materials Modeling, Freiburg, September 18-22, 2006, pg. 816.
17. M. Dobson, R. S. Elliott and E. B. Tadmor, "A Quasicontinuum for Complex Crystals", Proceedings of the Third International Conference on Multiscale Materials Modeling, Freiburg, September 18-22, 2006, pp. 889–896.